J. Physiol. (1978), 275, pp. 321-343
With 11 text-figures
Printed in Great Britain

FIRING BEHAVIOUR OF DORSAL SPINOCEREBELLAR TRACT NEURONES

BY B. GUSTAFSSON, S. LINDSTRÖM AND P. ZANGGER*
From the Department of Physiology, University of Göteborg, Göteborg, Sweden

(*Received 30 March 1977*)

SUMMARY

1. The repetitive discharge evoked by constant current injection from an intracellular micropipette has been studied in dorsal spinocerebellar tract cells of the cat.

2. The discharge frequency decreased with time, the decrease being more pronounced at high current intensities. Most of the frequency change occurred during the first ten intervals but the decrease continued slowly for several seconds. In some cells the frequency rose initially, the first interspike interval being larger than immediately succeeding ones.

3. The frequency–current (f/I) curves for the first interspike intervals were S-shaped, as found in spinal motoneurones. With successive intervals the lower leg of the f/I curve extended to higher frequencies, giving a progressive linearization of the f/I curves. In almost all cells this linearization was completed at 200 msec after current onset.

4. The experimental f/I curves were compared with the f/I curves obtained with a simple neurone model based on the properties of the postspike afterhyperpolarization. For the first interspike interval there was a good agreement between the experimental and calculated f/I curves of individual neurones up to frequencies of several hundred impulses per second. In the high frequency range, it was necessary to compensate for changes in initial postspike voltage trajectories caused by the injected current. Other aspects of the firing of real neurones, such as the progressive linearization of the f/I curves, the negative adaptation and the changes in the interspike voltage trajectories with increasing current were also reproduced by the neurone model.

5. It is concluded that the conductance process underlying the postspike afterhyperpolarization is a major factor in the regulation of repetitive firing in dorsal spinocerebellar tract neurones.

INTRODUCTION

An important function of the nerve cell soma is to translate a synaptic input into an action potential output of a given frequency. This translation mechanism has been analysed experimentally by the injection of controlled amounts of current into the cell soma from an intracellular micropipette. This approach is motivated by the fact that the synaptic and the injected current are activating the cell in the

* Present address: Institut de Physiologie, Université de Fribourg, Pérolles, 1700 Fribourg, Schweiz.

same way, namely by depolarizing the membrane of the initial segment (Eccles, 1957). A linear addition between the synaptic and the injected current has also been observed (Granit, Kernell & Lamarre, 1966*a*; Eide, Fedina, Jansen, Lundberg & Vyklický, 1969; Schwindt & Calvin, 1973*a*; see however Granit, Kernell & Lamarre, 1966*b*; Kernell, 1965*a*).

The repetitive firing evoked by injected current has been studied most extensively in cat spinal motoneurones (Kernell, 1965*b*, *c*, *d*; Schwindt & Calvin, 1972, 1973*b*; Schwindt, 1973; Baldissera & Gustafsson, 1974*b*, *c*). There is now good evidence that the firing of these neurones is controlled primarily by the longlasting afterhyperpolarization (a.h.p.), which follows each soma-dendritic spike (Kernell & Sjöholm, 1973; Baldissera & Gustafsson, 1974*b*, *c*; Baldissera, Gustafsson & Parmiggiani, 1977; Mauritz, Schlue, Richter & Nacimiento, 1974). In two preceding papers the a.h.p. properties of dorsal spinocerebellar tract (DSCT) neurones has been described in some detail (Gustafsson, Lindström & Takata, 1978; Gustafsson & Zangger, 1978). Since earlier observations indicated that the repetitive firing of DSCT cells differs from that of motoneurones (Kuno & Miyahara, 1968; Eide *et al.* 1969), the repetitive firing of DSCT cells evoked by current injection has now been re-investigated. It will be demonstrated that also in DSCT neurones the a.h.p. plays a decisive role for the regulation of repetitive firing. Preliminary reports of the present findings have been published (Gustafsson, Lindström & Takata, 1972; Gustafsson, 1974).

METHODS

The present material was collected in experiments fully described in a preceding paper (Gustafsson *et al.* 1978). Intracellular recordings were obtained from cat dorsal spinocerebellar tract (DSCT) neurones with single barrelled micropipettes filled with 2 M-potassium citrate or 3 M-potassium chloride. Experimental repetitive firing was studied in twenty-six neurones, selected from a larger sample for their stability. The repetitive firing was induced in these neurones by the injection of 500 msec long, depolarizing current pulses at a frequency of 0·2/sec. The current strength was changed stepwise from low to high values and back again several times and 4–6 current pulses were applied in succession at each intensity level. A stable sequence of measurements were then selected for the construction of the f/I curves. The repetitive firing of the model neurone (see Results, section V) was computed by a numerical solution of the differential equation with a third order Runge Kutta method, using a Hewlett-Packard calculator 9830 A. The time increment was 0·10 or 0·02 msec.

RESULTS

I. First interval frequency–current relationship

The frequency–current (f/I) relationship in DSCT neurones for the first interspike interval has been described previously as being upward convex over the whole frequency range (Kuno & Miyahara, 1968). This earlier analysis was somewhat incomplete, hardly covering frequencies below 100 impulses/sec, which is a serious limitation since DSCT neurones can fire regularly with a frequency down to 10–20 impulses/sec. A more complete f/I curve from a DSCT neurone is shown in Fig. 1 together with a sample of the interspike voltage trajectories. This upward concave–convex or sigmoidal curve was typical for all the eleven neurones where a similar large frequency range was covered and is similar to that described for spinal motoneurones (Granit, Kernell & Shortess, 1963; Kernell, 1965*b*; Baldissera &

Gustafsson, 1974*b*). In eight additional neurones, where only the frequency range below 600 impulses/sec was tested, all curves displayed an upward concave shape.

The *f/I* curve in Fig. 1*B* has been approximated by three straight lines. Although this procedure may seem justified for this cell, in other neurones the *f/I* curve

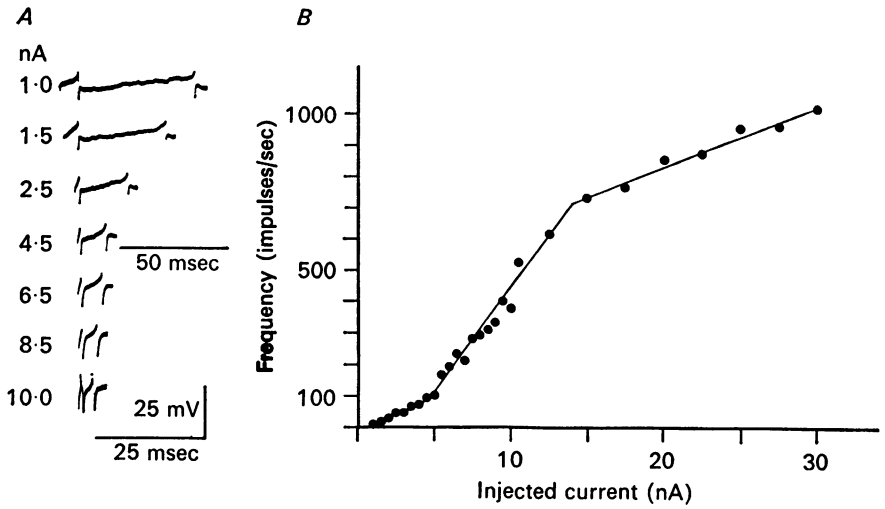

Fig. 1. First interval frequency–current relationship in a DSCT neurone. *A*, sample records of the first interval interspike voltage trajectories. *B*, the reciprocal of the first interval is plotted on the ordinate (impulses/sec) against the amount of injected current (nA = 10^{-9} A). Each point on the graph represents the average of 4–6 trials. The solid lines are fitted to the points by eye. Steady hyperpolarizing current 5 nA.

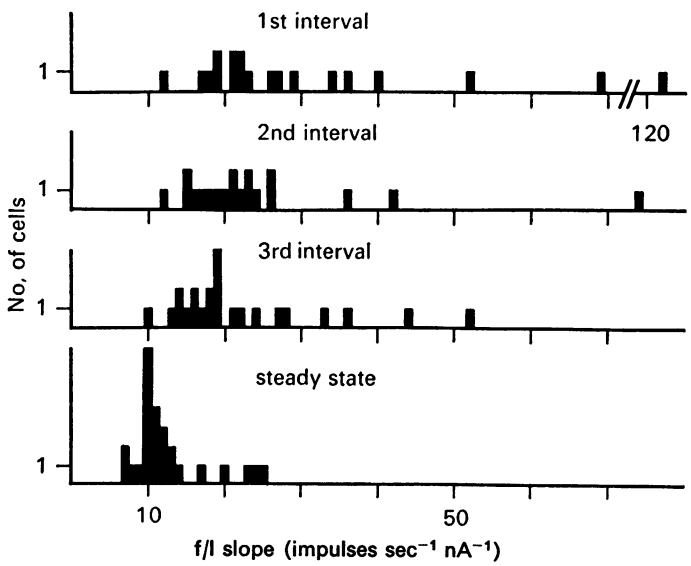

Fig. 2. Distribution of frequency–current slopes. The slope of the lower leg of the frequency–current (*f/I*) curves is indicated for different cells. The values for the first, second and third interval and for the 'steady-state' curves are shown separately. Further details in the text.

changed its slope in a more smooth and continuous manner, making such an approximation less attractive. However, for the purpose of giving quantitative data on the f/I relation, a similar approximation was made in all cells examined. The sigmoid f/I curve could then be characterized in an approximate way by the slopes and points of intersection of these lines. The slope of the lower leg of the curve was measured in nineteen neurones and the distribution of the values is given in the histogram in Fig. 2. Besides a few values above 40 impulses sec^{-1} nA^{-1} the slopes are concentrated between 15–30 impulses sec^{-1} nA^{-1}, which is 2–4 times steeper than in spinal motoneurones (Kernell, 1965*b*). The upward deviation of the f/I curve (measured as the point of intersection of the two lines) could be rather accurately measured in thirteen neurones and its distribution is shown in Fig. 3 (mean value 91 impulses/sec). In

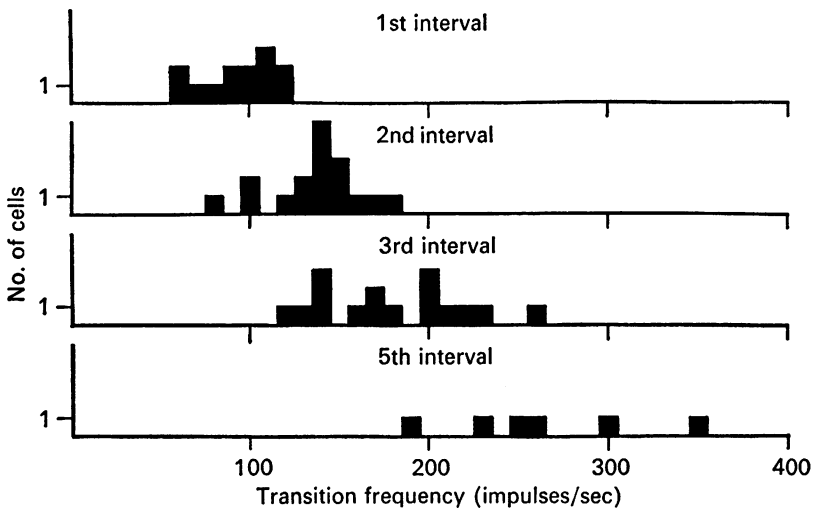

Fig. 3. Distribution of transition frequencies. The frequencies for the transition from the lower leg of the f/I curve to the steeper part in different cells are indicated for the first, second, third and fifth interspike intervals. Observe the gradual shift in transition frequency for the successive intervals, the lower leg of the curve extending up to 200–300 impulses/sec for the fifth interval.

all the cells examined the f/I curve proceeded smoothly from the lower leg of the curve into the steeper segment of the curve. Thus, in no case was there a sudden discontinuity or jump as found in some motoneurones (Baldissera & Gustafsson, 1974*b*). The difference in f/I slope between these two regions was also less than in motoneurones, the ratio being only 2·2 (n = 13) compared to around four in motoneurones (Kernell, 1965*c*). The transition to the upper leg of the f/I curve usually took place around 600 impulses/sec (mean value 627, range 350–900, n = 11). In this high frequency region the f/I slope was much the same for all the neurones examined, amounting to 20–25 impulses sec^{-1} nA^{-1}. The curve was followed above 1000 impulses/sec in five neurones without any appreciable decline in the slope.

II. First interval interspike voltage trajectories

The modifications of the interspike voltage trajectories with increasing amount of depolarizing current are illustrated by the records in Fig. 1*A* from a typical DSCT

neurone. In the subthreshold condition, the a.h.p. (starting from the peak of the delayed depolarization) displays first a fast hyperpolarizing phase, lasting a few milliseconds, which continues in a slower, shallow hyperpolarizing phase followed by a subsequent slow repolarization to the resting level (Gustafsson *et al.* 1978). From Fig. 1*A* it can be observed that already with a small current injection (1·0 nA), the hyperpolarizing portion is very much reduced. At this stage the trajectory is dominated by an almost linear, or in some cells an upward, weakly convex, repolarizing phase (cf. Fig. 8 in Gustafsson, 1974). The only modification introduced with increasing current is a reduction of the small concavity given by the hyperpolarizing phase and a gradual increase in the slope of the repolarizing phase. By comparing the interspike trajectories and the *f/I* curve it can be noted that there are no sudden changes in trajectory shape when passing from one segment of the *f/I* curve to the

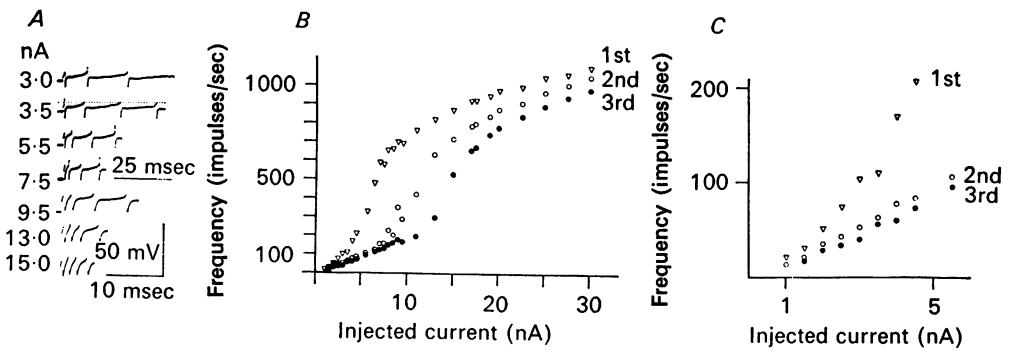

Fig. 4. Frequency–current relationship for the first three intervals in a DSCT cell without a.h.p. depression. *A*, sample records of the interspike voltage trajectories. The horizontal interrupted line in the 3·5 nA record represents the voltage level of the spike threshold; note in this and the following records that the postspike hyperpolarization is more pronounced during the second and third intervals than during the first. *B*, the reciprocals of the first (▽), second (○) and third (●) intervals are plotted on the ordinate against the amount of injected current. Each value represents the average of 4–6 trials. *C*, expansion of the initial part of the graph in *B*; no steady hyperpolarizing current.

next (see also Figs. 4 and 6 in this paper and Fig. 4 in Gustafsson, 1974). This smooth transition is to be expected from the continuous nature of the *f/I* curve. The upward convex shape dominating the trajectory at short intervals is given by the delayed depolarization and should not be confused with the inversion of the hyperpolarizing phase found in motoneurones (Schwindt & Calvin, 1972; Baldissera & Gustafsson, 1974*b*).

In Fig. 1*A* the second spike seems to take off at a more depolarized level than the first spike. This threshold elevation is presumably a recording artifact, due to resistance changes in the recording electrode during the current injection (note the similar change in the peak of the initial hyperpolarizing undershoot). In most other DSCT neurones there was no detectable change in the threshold level for the first few spikes (cf. Figs. 4 and 6).

III. Early adaptation

The frequency of firing evoked by constant current injection in DSCT cells is not constant, but decreases with time (Kuno & Miyahara, 1968; Eide *et al.* 1969). This frequency decrease or adaptation is most pronounced during the first few intervals but can last as long as 0·5 sec or more (Eide *et al.* 1969). Besides the adaptation, there is also for the successive intervals, a gradual change in the shape of the f/I

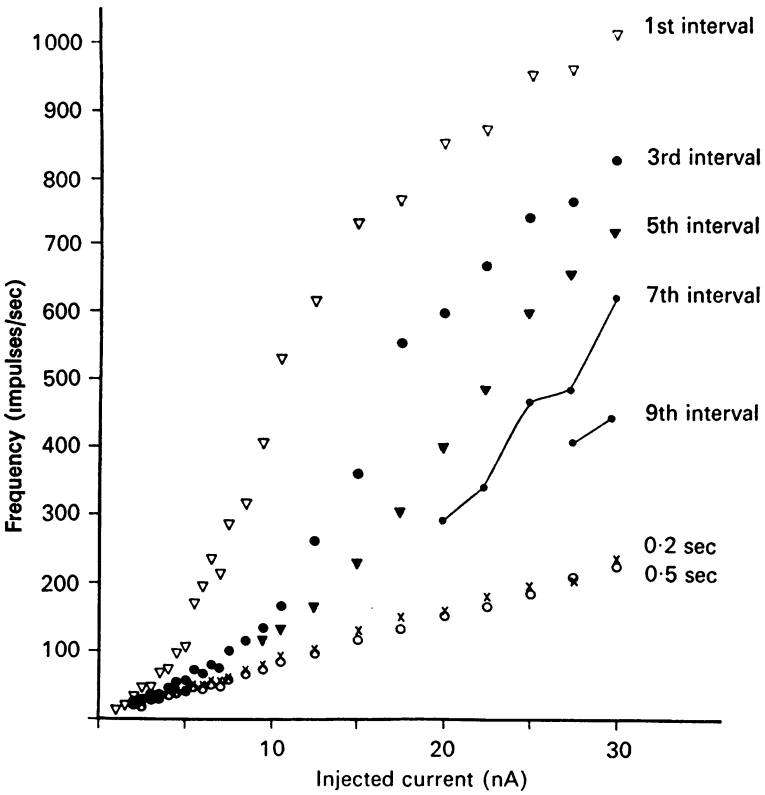

Fig. 5. Change in the frequency–current relationship from the first interval to the 'steady state'. Reciprocals of the first (▽), third (●) and fifth (▼) intervals after the current onset, together with the frequency at 0·2 sec (×) and 0·5 sec (○) are plotted against the amount of injected current. Inserted are also some measurements from the seventh and ninth intervals (small filled circles). Each point in the graph represents the average of 4–6 trials. The 0·2 and 0·5 sec values are the means of 2–3 successive intervals. Note that the main part of the adaptation from the first to the 0·5 sec interval has taken place within the first nine intervals (i.e. within the first 15 msec for the highest intensities). Steady hyperpolarizing current 5 nA.

curve. This change is illustrated for one neurone in Fig. 4 where the reciprocals of the first, second and third interval are plotted against the injected current. The f/I curves for the later intervals also display a sigmoid shape but there is an extension of the lower leg of the curve to higher frequencies, giving an almost linear f/I relation for the third interval up to about 200 impulses/sec. The transition level between the lower and middle segment of the f/I curves was measured for the second, third and

fifth interval and the resulting values are given in Fig. 3. There was a gradual increase in the mean values of the transition frequency from around 90 impulses/sec (first interval) to values of 134, 176 and 261 for the second, third and fifth intervals respectively.

A similar change in f/I curves over a longer time period is illustrated in Fig. 5. Observe here the continued increase in transition level from the third interval curve to the 0·2 and 0·5 sec interval curves, the latter f/I curves extending linearly above 200 impulses/sec. This gradual linearization of the f/I curve with successive intervals is in agreement with the finding of Eide *et al.* (1969) of a single linear f/I relation in DSCT cells when studied in 'steady state', i.e. after the initial adaptation is completed (see below). They found that this linearity in some cells could extend up to 600 impulses/sec before the slope started to decrease. In the present study only two cells were followed, at the 0·5 sec interval, up to a frequency level where the slope started to decrease, i.e. reached the upper leg of the f/I curve. In both cells, this level (340 and 450 impulses/sec) was reached with a linear f/I curve, not showing any tendency to an upward deviation. Of twenty three cells in which the 0·5 sec interval f/I curve was extended beyond 100 impulses/sec an upward deviation was found in only two cells. The transition frequencies of these cells were 140 and 230 impulses/sec and the slope ratios were 1·5 and 2·6 respectively. In the remaining twenty-one neurones the f/I curve extended beyond 200 impulses/sec in eleven cells, beyond 300 in four cells and beyond 400 impulses/sec in three cells without displaying an upward deviation.

While this change in the f/I curve shape during the initial adaptation was common for all the neurones examined, a more intricate relation between the first few interspike intervals was found in several cells. In fact, of twelve cells where the first three interspike intervals were followed in a reasonably large frequency range, only six cells behaved similarly to that shown in Fig. 4. In these cells there was a clear decrease in slope from the first to the second interval for the lower leg of the f/I curve (mean 1st/2nd f/I slope ratio 1·5; cf. Fig. 10*D*, filled circles). There was also a large shift to the right of the remaining part of the f/I curves for the later intervals. In five neurones the f/I curves behaved more like that illustrated in Fig. 6. In this neurone, there is no apparent change in slope of the lower leg of the curve for the first and second interval (cf. Fig. 10*D* open circles), the curve for later interval is merely shifted to the right (Fig. 6*B*, *D*). After the upward deviation the f/I slope is steeper for the later intervals than for the first leading to an intersection of the curves. Thus at high current intensities there is an initial increase in frequency, i.e. a negative adaptation. The intersection of the first and second interval curves occurred in the five neurones at various levels, ranging from 180–450 impulses/sec. In two neurones, the first and the third interval curves also intersected at a somewhat higher frequency, 390 and 490 impulses/sec. Since the third interval slope was steeper than the first interval slope also for the three remaining cells, where no crossing was seen (Fig. 6*B*), it is likely that a crossing would have occurred if higher current intensities had been tried. In one of these neurones there was also a negative adaptation at low current intensities, with the second interval curve to the left of the first interval curve at frequencies below 100 impulses/sec (see Fig. 9, Gustafsson, 1974). Thus, this cell had a second interval curve which intersected the first interval

curve twice, with a 1st/2nd interval slope ratio for the lower leg of less than 1 (lowermost open circle in Fig. 10 *D*). In the remaining neurone no negative adaptation was found in spite of a low 1st/2nd interval slope ratio (1·12). In all cells examined there was a small decrease in f/I slope between the second and third interval, the ratio being 1·16 (mean value, $n = 19$). In none of the cells was there an intersection of the second and third interval curves as has been described for motoneurones (Baldissera & Gustafsson, 1974*c*).

The differences in adaptation illustrated by the f/I curves in Fig. 4 and 6 were

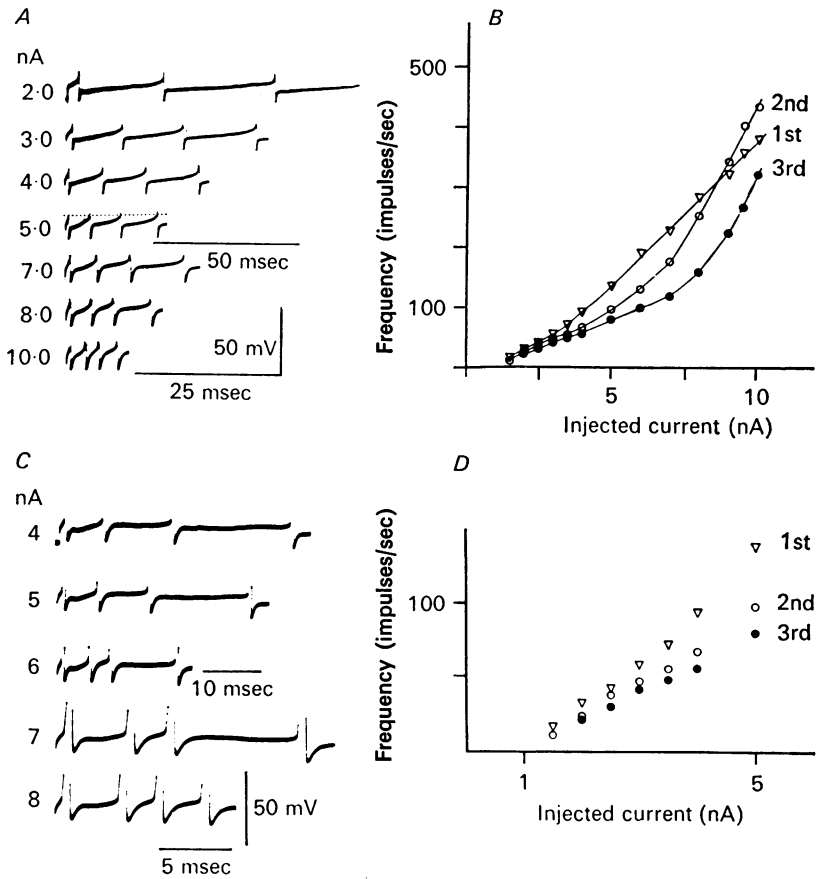

Fig. 6. Frequency–current relationship for the first three intervals in a DSCT cell with a.h.p. depression. *A*, sample records of the interspike voltage trajectories; in the 5·0 nA record a horizontal interrupted line is drawn as in Fig. 4; note the somewhat smaller hyperpolarization during the second than during the first interval trajectory. *B*, the reciprocals of the first (▽), second (○) and third (●) intervals are plotted against the amount of injected current; note the intersection of the second and first interval curves at high frequency. *C*, sample records from another DSCT neurone with a.h.p. depression; at some current intensities the first interval is longer than the second (6–8 nA) and the third (8 nA) intervals; observe that the initial concavity (after the delayed depolarization peak) is more pronounced in the first interval trajectory than in the succeeding ones. *D*, expansion of the initial part of the graph in *B*. Each value in *B* and *D* represents the average of 4–6 trials. Steady hyperpolarizing current 14 nA.

also reflected in the interspike voltage trajectories. In the group with a clear adaptation the hyperpolarizing phase was more pronounced for the later intervals than for the first at all current intensities except the lowest (Fig. 4*A*). In the other group the hyperpolarizing phase was more shallow for the later intervals than for the first, even in the presence of an adaptation (Fig. 6*A*). Just before the intersection of the *f*/*I* curves the trajectory was in some cells almost flat for the later intervals (6 and 7 nA in Fig. 6*C*; Fig. 9 in Gustafsson, 1974).

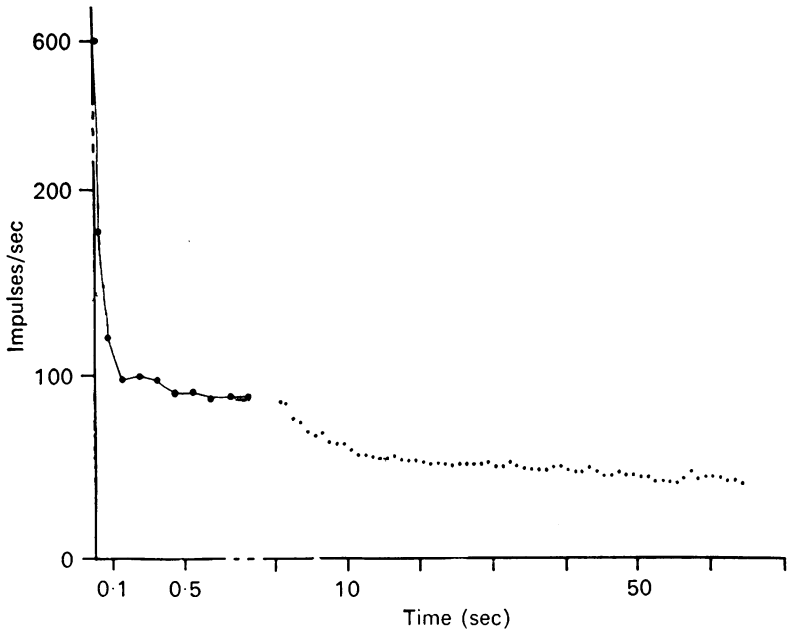

Fig. 7. Late adaptation. The frequency at one current strength is measured from the first interval to 65 sec after the current onset. The filled circles represents from the left the reciprocal of the first (at 600 imp/s) and second intervals (at 180 imp/s), the mean frequency between 50–100 ms after current onset and the mean frequency during the succeeding 100 ms periods. The dots represent the mean frequency during one second periods with the measurements beginning one second after current onset. The ordinate is interrupted between 200 and 600 imp/s and two different time bases are used for the abscissa.

IV. Late adaptation

Since the adaptation in DSCT neurones can last 0·5 sec or more (Eide *et al.* 1969), the *f*/*I* relationship was also determined at 0·2 and 0·5 sec after the current onset. As can be observed in Fig. 5 there is a further change in the slope of the lower leg of the *f*/*I* curve, when going from the third to the 0·2 sec interval. For twenty-three neurones this *f*/*I* slope ratio (third/0·2 sec) varied between 1·4 and 2·5 with a mean value of 1·8. On the other hand, there was no apparent slope change from 0·2–0·5 sec, which was true for all the ten neurones where this comparison was made. The slope measured at 0·2 and 0·5 sec can then be considered as a steady state slope and the distribution of the measured values are given in Fig. 2. The values were found to vary between 7·2 and 25·4 impulses sec^{-1} nA^{-1} with a mean value of 12·7

($n = 26$). This mean value for the steady state current–frequency relationship is about twice that given earlier for DSCT neurones from a smaller sample (Eide *et al.* 1969) and is about six times the average value given for spinal motoneurones (Kernell, 1965*c*).

The decrease in frequency with time was not completed within 0·2 seconds. In many of the cells, there was a further adaptation to the 0·5 sec interval, corresponding to a parallel shift of the f/I curve to the right. In the ten neurones examined, this shift of the curves along the abscissa was equivalent to 0 to 2·0 nA of injected current with a mean value of 0·9 nA. In three neurones the firing was followed to 30–60 sec after the current onset, during which time a further continuous decrease in frequency could be observed. This is illustrated for one cell in Fig. 7 where the frequency at one current strength is plotted against time after current onset. After an initial fast frequency decay during the first 10 sec there is a rather linear decay with a slope of 0·25 impulses sec^{-1} sec^{-1}. In the other two cells the slopes of the late adaptation were 0·46 and 0·68 impulses sec^{-1} sec^{-1}. Since only one current strength was used in each cell, it could not be determined whether this phase of the adaptation continued without a change in slope, as does the similar longlasting adaptation described in motoneurones (Granit, Kernell & Shortess, 1963).

Although a real steady state of repetitive firing was not achieved during constant current injection in the DSCT neurones it should be stressed that the predominant part of the frequency decrease occurred during the first few intervals. For the cell in Fig. 5 the frequency at 30 nA decreased from 1016 impulses/sec for the 1st interval to 440 for the 9th interval and to 235 impulses/sec for the 0·2 sec interval. Thus, 74% of the adaptation was completed within the first nine intervals. Similar calculations made in six additional neurones, at a current strength where the 0·2 sec frequency was around 200 impulses/sec, gave adaptation values of 69–92% (mean value 81%). The same point can be made from Fig. 7. In this cell about 90% of total adaptation during 60 sec of repetitive firing occurred during the first 150 msec. The adaptation rate during this first phase was about 3500 impulses sec^{-1} sec^{-1} as compared to 0·25 impulses sec^{-1} sec^{-1} during the late adaptation phase.

V. A DSCT model neurone

As first discussed by Adrian & Zotterman (1926; cf. also Kernell, 1968) the frequency–current relationship of neurones could be controlled by the time course of the refractoriness following each spike. According to this model the next spike will be evoked whenever the current injected is sufficient to counteract the refractoriness created by the preceding spike. Thus, if the magnitude and the time course of the refractoriness following each spike is known, the relation between current and interspike intervals (or frequency) could be predicted.

In central neurones (e.g. motoneurones and DSCT neurones) the postspike refractoriness is due primarily to the a.h.p., except at short intervals just after the spike. In two preceding papers the a.h.p. properties of DSCT neurones were described (Gustafsson *et al.* 1978; Gustafsson & Zangger, 1978). In order to evaluate the role of the a.h.p. in the regulation of the firing of DSCT neurones, a neurone model based on these a.h.p. properties has been formulated. For simplicity the complex geometry of the neurone is neglected, and the neurone is treated as sphere. Apart

from the a.h.p. all other neurone parameters are kept constant. These include the threshold voltage for spike initiation, the spike duration, the voltage level reached by the falling phase of the spike (initial undershoot), the delayed depolarization and all other conductances and their equilibrium potentials (throughout the interspike interval).

The a.h.p. properties used in the model can be described as follows:

(1) The potassium conductance underlying the a.h.p. is potential independent at levels more negative than the threshold voltage, and has a time course as described in a preceding paper (Gustafsson *et al.* 1978).

(2) The a.h.p. conductance evoked by each spike is unaffected by the succeeding spikes; i.e. there is a linear superposition of successive a.h.p.s (Gustafsson & Zangger, 1978).

(3) The a.h.p. conductance evoked by the second and succeeding spikes after the onset of the constant current pulse is a constant fraction (a) of the a.h.p. conductance evoked by the first spike (to allow for the introduction of a.h.p. depression; Gustafsson & Zangger, 1978).

In the model a new spike is generated whenever the voltage trajectory following the preceding spike intersects the constant spike threshold voltage. The interspike voltage trajectory can be calculated using the differential equation:

$$G_{\mathrm{ahp}}(t) \times (V_{\mathrm{ahp}} - V(t)) - G_L \times V(t) - C \times \frac{\mathrm{d}V(t)}{\mathrm{d}t} - I - DD(t) = 0 \qquad (1)$$

where

$G_{\mathrm{ahp}}(t)$ = time course of the conductance underlying the a.h.p. (eqn. (3) in Gustafsson *et al.* 1978).

$DD(t)$ = time course of the depolarizing current underlying the delayed depolarization (eqn. (4) in Gustafsson *et al.* 1978).

C = input capacitance,

G_L = leakage or resting input conductance,

V_{ahp} = difference (positive value) between the threshold voltage and the a.h.p. equilibrium potential,

$V(t)$ = difference (positive value) between the threshold voltage and the a.h.p. voltage,

I = injected current exceeding the rheobase.

Eqn (1) can be solved numerically in $V(t)$ for step increases of I. The solutions are the a.h.p. trajectories corresponding to different amounts of injected current. By measuring the time at which the a.h.p. voltage intersects the threshold voltage for spike initiation, i.e. the time at which a second spike would appear, one can compute from the same equation the f/I relation for the first interspike interval. The computations are started at a fixed voltage level below threshold corresponding to the peak level of the initial undershoot (see above). Computations are started 0·5 msec after the onset of the spike so as to allow for the spike duration.

To obtain the f/I curve for the second interval, the a.h.p. conductance remaining from the first spike is added to the conductance started by the second spike. The value of the a.h.p. conductance given by the second spike is equal to $a \times G_{\mathrm{ahp}}(t)$

where a is a proportionality factor ($\leqslant 1$) which is constant for each computation. The new conductance $G_{ahp}(t+t_1)+a \times G_{ahp}(t)$ (t_1 = duration of the first interval) determines the trajectory of the second a.h.p. The second interval is then measured and the computation can be continued for the desired number of intervals, each new $G_{ahp}(t)$ being multiplied by a.

VI. Frequency–current relationship of the model neurone

The results of two computations of the first three interval f/I curves and the trajectory are shown in Figs. 8 and 9. The value of a was set to 1·0 in Fig. 8 and 0·6 in Fig. 9. Thus, these two figures represent the firing given by a model with a linear a.h.p. summation (Fig. 8), and that given by a model with a clear a.h.p.

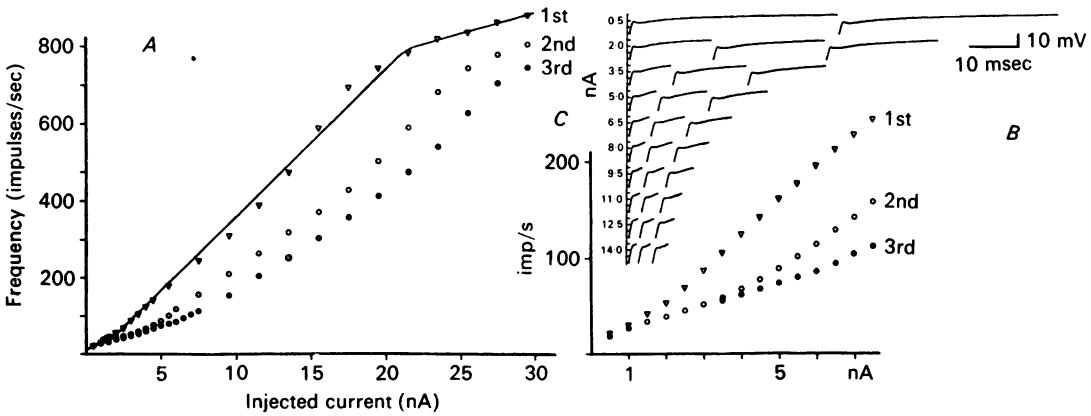

Fig. 8. Frequency–current relationship of a DSCT model without a.h.p. depression. *A*, the reciprocals of the first (▽), second (○) and third (●) interspike intervals obtained with the model are plotted against the amount of injected current; the model is described in detail in the text. The values of the parameters in the expressions for the a.h.p. conductance and delayed depolarization current were, with three exceptions, the same as those used for the computed a.h.p. in Gustafsson *et al.* 1978, Fig. 9; the A_1 value was changed from 0·75 to 0·85, the B_1 value from 0·16 to 0·14 and the K_1 value from 43 to 58; this gave small changes in the magnitudes of the $G_{ahp}(t)$ and $DD(t)$ expressions without changes in their time course; the calculations were started at t = 0·5 msec, at a fixed voltage level 15 mV below the threshold, and the value of a was 1. *B*, interspike voltage trajectories given by the model. *C*, expansion of the initial part of the plot in *A*.

depression (Fig. 9; also Gustafsson & Zangger, 1978). The cell parameters inserted in eqn. (1), and the values given to the constants in the expressions for $G_{ahp}(t)$, and $DD(t)$, are given in the legend to Fig. 8. The shape of the $G_{ahp}(t)$, and $DD(t)$ curves given by these values has previously been shown (Fig. 9 in Gustafsson *et al.* 1978).

The computed first interval curve has an upward concave–convex or sigmoid shape, as observed in the real neurones. This shape was substantially independent of the $G_{ahp}(t)$ and $DD(t)$ parameters. Changing the DD current or the magnitude of the initial fast $G_{ahp}(t)$ phase merely changed the slope of the steep part of the curve, or the transition level to the upper leg, without affecting the general sigmoid shape. Without 'delayed depolarization' current the f/I curve could almost be linear (see Fig. 3, Gustafsson, 1974).

The slope of the lower leg of the f/I curve was 21 impulses/sec. As expected this slope was determined by the magnitude of the $G_{ahp}(t)$. The frequency for transitions from the lower leg of the curve to the middle phase was dependent upon the time constant for the slow $G_{ahp}(t)$ decay, and was 70, 55 and 50 impulses/sec for time constants of 14, 20 and 26 msec respectively. This is within the range found for real DSCT neurones. The slope of the steep part of the first interval curve was 38 impulses sec^{-1} nA^{-1} and the transition to the upper leg was at 800 impulses/sec, also within the range of values found for the real neurones (cf. section I). Note that with the chosen values for the constants in the $G_{ahp}(t)$ and $DD(t)$ expressions, the steep part of the model f/I curve is not quite linear. Similar non-linearities were observed also in real DSCT neurones (see sections I and II).

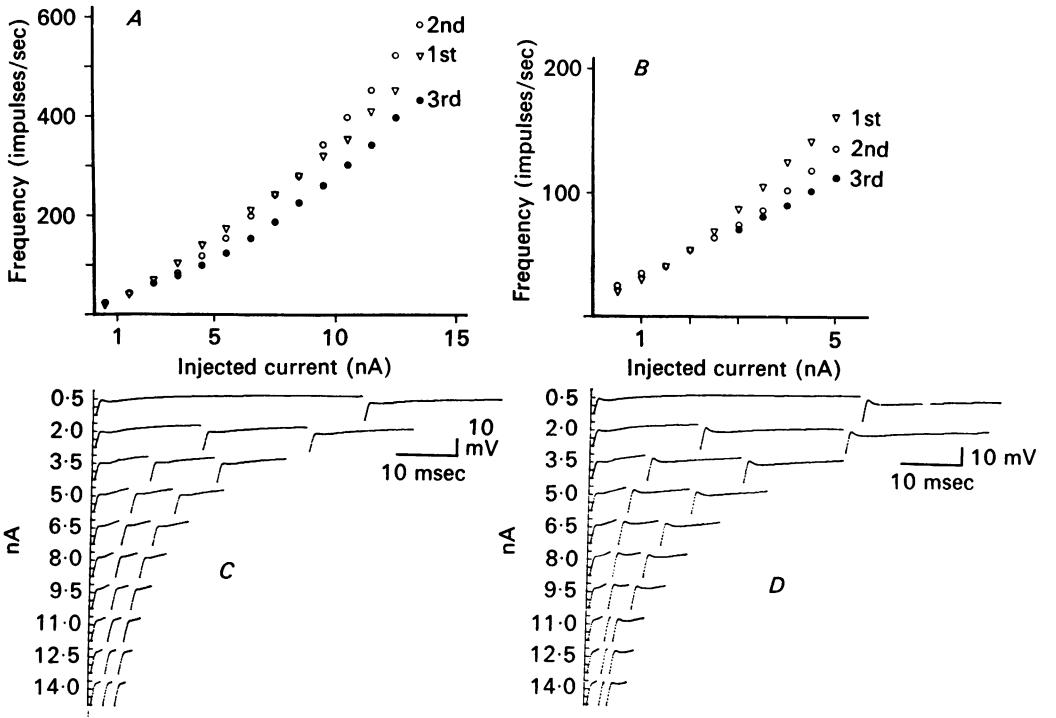

Fig. 9. Frequency–current relationship of a DSCT model with a.h.p. depression. *A*, *B*, data from the same model as in Fig. 8 but using an a value of 0·6; note that the second interval f/I curve is displaced to the left of the first interval curve at low frequencies (*B*) and at high frequencies (*A*), i.e. that there is an initial negative adaptation; further details in the text. *C*, interspike voltage trajectories given by the model version in *A*. *D*, interspike voltage trajectories given by a model version without a.h.p. depression ($a = 1$) but with the delayed depolarization current increased 40 % from the first to the second spike. Also this model gives a negative adaptation in the high frequency range (9·5–14 nA). Note the increase of the hyperpolarization in the interspike voltage trajectories from the first to the second interval at low frequencies.

In both versions of the model, there is an upward extension of the lower leg of the curve at later intervals, i.e. an increased linearization of the f/I curve with successive intervals. For the two model versions the lower leg increased from 55 impulses/sec for the first interval to 85 and 110 (no depression) and to 110 and 140 impulses/sec

(depression) for the second and third intervals respectively. The magnitude of this increase was rather independent of the time constant of the $G_{ahp}(t)$ decay, the absolute frequency for the transition levels shifting upwards with a faster decay and vice versa (cf. above). The linearization of the model f/I curves was not completed within the third interval. In fact, the computed f/I curves for later intervals would become successively linearized until a single linear steady-state f/I curve is reached. This development of a linear steady-state f/I relation from algebraically summating exponential $G_{ahp}(t)$ decays has previously been demonstrated by MacGregor & Sharpless (1973) and Baldissera & Gustafsson (1974*c*).

In the model with a linear summation and no depression, there was also a decrease in the slope of the lower leg of the curve from the first to the second interval. This slope ratio was around 1·7, and was little affected by changes in the time constant of the slow $G_{ahp}(t)$ decay (14–26 msec). In this model version there was also a large shift to the right of the steeper part of the curve for the later intervals, as happens in real neurones (cf. Fig. 4). With the inclusion of depression (Fig. 9), the second and third interval f/I curves had a similar slope, but were displaced to the left of the first interval curve at low frequencies. A similar negative adaptation was found in one DSCT neurone in this frequency range (section III). After the upward deviation from the lower leg of the curve, the slopes were steeper for the later intervals than for the first, giving an intersection of the first and second interval f/I curves. In some model versions the first and third interval curves intersected (cf. Fig. 7, Gustafsson, 1974) at high frequencies, showing a negative adaptation, as observed in some DSCT neurones (cf. Fig. 6).

In both model versions there is a slight decrease in f/I slope from the second to the third interval with a ratio about 1·1. From the third interval onwards, the model shows no evidence of rotation or change in slope of the f/I curve, adaptation being seen only as an upward extending linearization of the curve. In this respect the model differs from DSCT neurones where a further slope change could be observed between the third and the 0·2 sec interval curves.

VII. Interspike voltage trajectories of the model neurone

The modifications in the computed interspike voltage trajectories with increasing current injection (Fig. 8*B* and 9*C*) were much the same as those observed in real DSCT neurones. The main change with increasing current was an increase in the slope of the repolarizing phase, together with a gradual reduction of the small hyperpolarizing concavity. At short intervals the trajectory was dominated by the upward convexity given by the 'delayed depolarization', as in real neurones. It can be observed that the different computed adaptation patterns in 8*A* and 9*A* are associated with different trajectory behaviour. As in real neurones, an adaptation is associated with an increase of the hyperpolarizing phase for the later intervals (Fig. 8*B*). On the other hand, the hyperpolarization produced by depression is less pronounced for the later intervals, even in the presence of an adaptation (3·5–5 nA in Fig. 9*C*).

A negative adaptation in the high frequency range, similar to that in Figs. 6 and 9 could also be produced by the model without a.h.p. depression, provided that the $DD(t)$ current was markedly increased. However, in this version the model inter-

spike trajectories differed from the trajectories in the model version with a.h.p. depression, and from those of the real DSCT neurones. This is illustrated by the computed trajectories in Fig. 9*D*. Note that with an increase in delayed depolarization, the concavity given by the hyperpolarizing phase is more pronounced for the later intervals than for the first one (e.g. 2–5 nA in Fig. 9*D*), whilst the reverse is true for the real neurones (Fig. 6).

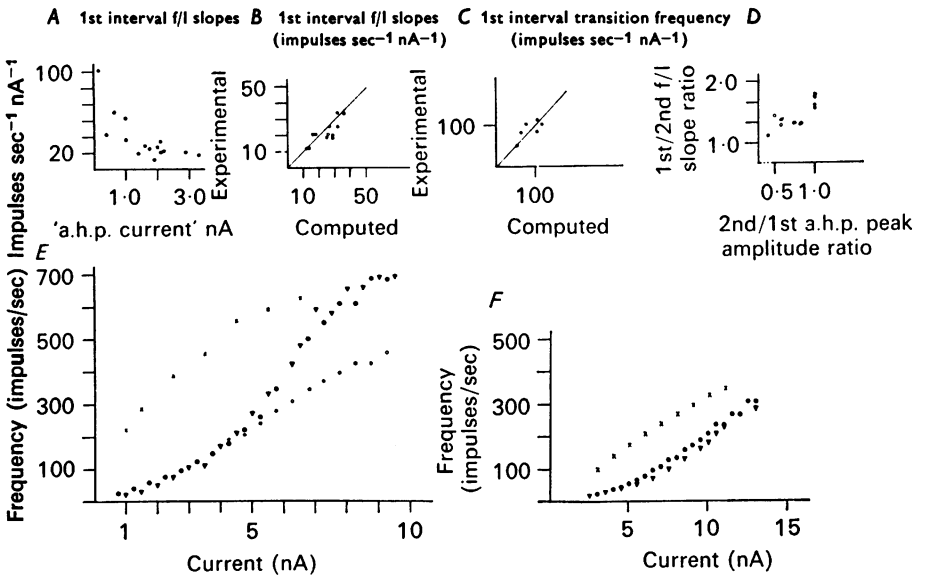

Fig. 10. Comparison between a.h.p. and f/I curves. *A*, relationship between the slope of the lower leg of the first interval f/I curve and the a.h.p. 'peak current' for fifteen neurones. *B*, relationship between the slope of the lower leg of the experimental first interval (f/I) curve (ordinate) and the corresponding slope for the f/I curve calculated from the a.h.p. conductance in the same cells (abscissa). The a.h.p. reversal level was estimated to 15 mV (○) and 20 mV (●) below the holding potential. The drawn line indicates equivalence between the experimental and calculated f/I slopes. *C*, relationship between the frequency of transition from the lower leg to the steeper part in the experimental (ordinate) and the calculated f/I curves (abscissa), obtained as in *B*; for the calculated curves the a.h.p. reversal level was assumed to be 20 mV below the holding potential; the drawn line indicates equivalence between the experimental and calculated values. *D*, relationship between the change in the slope of the lower leg of the f/I curve from the first to the second interval and the amount of a.h.p. depression. ○, cells with depression; ●, cells without depression. Note that in cells with an a.h.p. depression the slope change is small or absent. *E*, *F*, comparison between the experimental first interval f/I curve (▼) and the f/I curve calculated from the a.h.p. conductance in the same cell (●). Two different DSCT neurones. ○, values obtained with a fixed voltage level for the starting point of the computations, 3·7 mV below the threshold voltage; ×, values given by the passive membrane properties. The a.h.p. reversal level was assumed to be 20 mV below the holding potential. The input resistance and capacitance were 1·2, 2·6 MΩ and 1·4, 2·1 nF for the cell in *E* and *F* respectively. Further details in the text.

VIII. Comparison between afterhyperpolarization and f/I curve in individual cells

In fifteen neurones the current produced by the a.h.p. following a single spike was estimated by dividing the a.h.p. peak amplitude by the input resistance of the

neurone. This 'a.h.p. current' was then related to the slope of the lower leg of the f/I curve for the first interval in the same cell. As shown in Fig. 10*A*, there was a negative correlation between the f/I slope and the magnitude of the 'a.h.p. current', as would be expected if the firing was controlled by the a.h.p.

A more direct quantitative comparison between the a.h.p. and the f/I curve was performed in six of the above neurones. For these cells the time course of the a.h.p. conductance was calculated from the a.h.p. voltage following a single spike (as described by Gustafsson *et al.* 1978). The calculations were performed with estimated a.h.p. reversal levels 15 and 20 mV more negative than the holding potential (Gustafsson *et al.* 1978). The resulting conductance time course was then inserted into eqn (1) (section V), replacing the model conductance time course ($G_{ahp}(t)$) previously used. For computation of the firing, the driving force for the a.h.p. was increased with the difference between the holding potential and the threshold voltage for spike initiation in the actual cell. The early part of the calculated a.h.p. conductance is influenced to an unknown degree by the current underlying the delayed depolarization. On the assumption that the delayed depolarization current is shortlasting (cf. Gustafsson *et al.* 1978) the computations were started shortly after the peak of the delayed depolarization (1–3 msec after spike onset) and the $DD(t)$ factor in eqn. (1) was omitted. At these intervals following the spike onset the voltage level of the starting point was not unaffected by the injected current in real neurones, but was displaced in a depolarizing direction with increasing current. To account for this shift, both the voltage level of the starting point at threshold current, and its displacement with increasing current, were measured in the real cell and introduced into eqn (1). Other parameters in eqn (1) were also taken from the actual cell.

The experimental (▲) and the computed (●) f/I curves for the first interval are shown for two neurones in Fig. 10*E* and *F*. Note that the experimental and calculated curves are quite similar in shape and overlap over the whole frequency range. Fig. 10*B* shows plots of the f/I slope for the lower leg of the experimental curves for all six neurones, compared with the computed curve, using a.h.p. reversal levels 15 (○) and 20 (●) mV below the holding potential. There is a reasonable agreement between the slope of the experimental and computed curves, and this correspondence was little affected by the selected a.h.p. reversal level. The frequencies at which the experimental and calculated curves begin to deviate upwards are plotted against each other in Fig. 10*C*, and show a similarly good correlation.

The use of the actual voltage level in the cell as the initial value for the computations leads necessarily to an agreement between the experimental and calculated curves when the starting point reaches the threshold. The similarity between the curves at the highest frequency is thus of no significance as concerns the role of the a.h.p. in the firing regulation. At this high frequency, the factors controlling the early trajectory and consequently the starting voltage; the a.h.p. conductance, the delayed depolarization current, the spike conductances and the passive membrane properties are all likely to be involved in the firing control. The degree of fit between the experimental and calculated curves at frequencies lower than this, would, however, indicate the importance of the a.h.p. after taking into account the early trajectory changes. The f/I curve obtained with a constant voltage level of the starting point 3·7 mV below threshold, which was equal to the value at threshold current,

is shown by open circles in Fig. 10*E*. The calculated *f/I* curve was unaffected by this change in the initial values at frequencies below 200 impulses/sec. This was also true when the starting voltage was fixed to 0·5 mV below threshold. Thus, at these lower frequencies the interspike intervals seem to be exclusively controlled by the a.h.p. conductance.

The experimental *f/I* curves were also compared with those given by the passive membrane properties alone. In this case, the calculations were started at the same time as in the previous example and the starting voltage level was shifted as in the real cell. Thereafter, the rise to the threshold voltage was determined exclusively by the resting input capacitance and resistance. The resulting *f/I* curve is shown by crosses in 10*E* and *F* and displays an upward convex shape with a considerably steeper slope than the experimental one. Observe that even if the two curves are aligned at the highest frequency where the starting point crosses the threshold level, they differ over most of the high-frequency range. This indicates that the a.h.p. conductance is also of importance for firing regulation in this range.

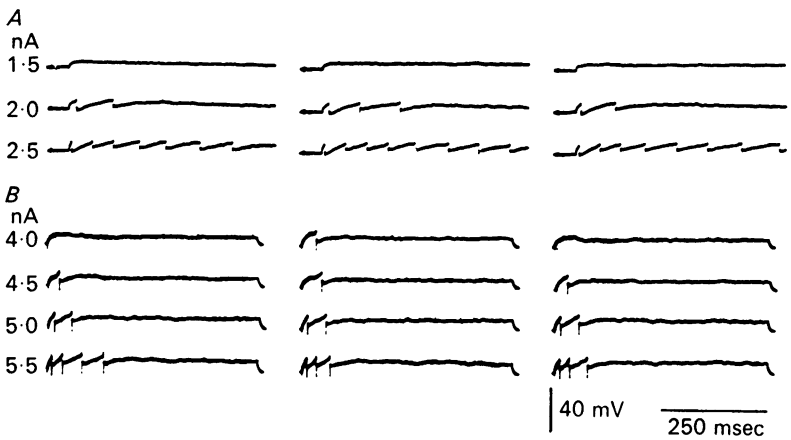

Fig. 11. Threshold current differences for the first few spikes. *A* and *B* are from two different DSCT neurones. For each cell three successive sweeps at current strengths close to the threshold level are shown.

The shape of the *f/I* curves for the second and third interspike intervals in relation to the first, varied considerably between different DSCT neurones (section II). In some neurones there was a small slope change from the first to the second interval, combined with an intersection of the *f/I* curves at high frequency. The same behaviour of the computed *f/I* curves was obtained when an a.h.p. depression was introduced into the model (section VI). To determine whether a.h.p. depression was in fact responsible for this behaviour in the real neurones, the incidence of a.h.p. depression was studied in ten of the neurones with complete *f/I* curves. Five of these neurones had a small change in the *f/I* slope and an intersection of the curves at high frequency. All five cells displayed a clear a.h.p. depression when the a.h.p. interaction was studied at long intervals (Gustafsson & Zangger, 1978). An additional cell with a small *f/I* slope change, but without negative adaptation in the high frequency range, also showed a.h.p. depression. On the other hand, there was no detectable depression in the remaining four neurones, which all had a clear *f/I* slope

change and no negative adaptation. The correlation between small f/I slope ratio and a.h.p. depression is illustrated in Fig. 10*D*, where the ratio between the slopes of the f/I curves for the first and second interval is plotted against the ratio between the second and first a.h.p. peak amplitude, measured at an interspike interval equal to the a.h.p. duration (Gustafsson & Zangger, 1978).

Only in one cell with depression was there a negative adaptation at low frequencies (section III) as seen in the model. In the remaining cells with depression, the second a.h.p. was smaller than the first one at long intervals. Therefore, other factors must be responsible for the adaptation at low frequencies in these cells. It has been demonstrated for motoneurones that more current is needed to evoke repetitive firing than to evoke a single spike (Baldissera & Gustafsson, 1974*b*). A similar difference in threshold current has been observed also in DSCT neurones, as exemplified by two neurones with a.h.p. depression in Fig. 11. In this figure three successive sweeps with the same current strength are shown in each row. For the neurone in *A*, the threshold difference was rather small (less than 0·5 nA between the first and third spike) whilst the difference was more pronounced for the cell in *B*. In the latter cell the current had to be increased by more than 1 nA to evoke the third spike and by more than 1·5 nA for continuous repetitive activity. A shift to the right of the second interval curve of about 0·5 nA would be enough to eliminate the negative adaptation at low frequencies in cells with depression (cf. Figs. 6*D* and 9*B*). Therefore, it is possible that the lack of negative adaptation in these cells is due to the observed change in threshold current for later spikes. In line with this notion is the finding that the cell in Fig. 11*A* with a small threshold difference also had a negative adaptation at low frequencies.

In motoneurones the voltage change induced by a subthreshold constant current pulse declines with time (Ito & Oshima, 1965). It has been suggested (Baldissera & Gustafsson, 1974*b*) that this 'sag' phenomenon, rather than an increase in the threshold voltage for spike initiation, is responsible for threshold changes shown in Fig. 11. The 'sag' behaviour has been demonstrated previously in DSCT neurones (Kuno & Miyahara, 1968) and is visible in the records in Fig. 11*B*. As mentioned before (section II) there were usually no detectable changes in the threshold voltage for the first few spikes in the DSCT cells. Therefore, the 'sag' phenomenon might be responsible for the observed threshold differences in DSCT neurones.

DISCUSSION

The present results demonstrate that the firing behaviour of the dorsal spinocerebellar tract neurones is substantially similar to that of cat spinal motoneurones, the only central neurones studied in detail previously (for ref. see Introduction). They also suggest that the repetitive firing in DSCT cells, as in motoneurones, is mainly governed by the kinetics of the conductance process underlying the a.h.p.

Direct evidence for the role of the a.h.p. in the firing regulation was the good correlation between the experimental f/I curve for the first interspike interval and the f/I curve obtained with a model based on the a.h.p. conductance in the same cells. By necessity, this comparison was based on several simplifying assumptions both in the calculations of the a.h.p. conductance, and in the computations of the f/I curve. The a.h.p. was assumed to be due to a single conductance process, which was

unaffected by subthreshold displacements of the membrane potential. Although this has not been proven conclusively, the findings of Gustafsson *et al.* (1978) indicates that this is a reasonable approximation. The reversal level for the a.h.p. was not determined experimentally, but was assumed to be 20 mV below the holding potential (Gustafsson *et al.* 1978). However, reasonable changes in the value of the reversal level gave only minor changes in the calculated curves (Fig. 10*B*). Furthermore, the complex geometry of the neurone was neglected, and the neurone treated as a sphere, both for the calculations of the a.h.p. conductance and for the firing computations. This simplification was used since the spatial distribution of the a.h.p. conductance is not known, but it would probably not introduce any serious error. If the a.h.p. is evoked only in the soma membrane, the a.h.p. current and the injected current would be distributed in the same way and the above simplification justified. Only at high frequencies (above 200–300 impulses/sec) will the calculated and experimental f/I curves deviate due to the overestimation of the a.h.p. conductance in its initial part (Gustafsson *et al.* 1978). The experimental f/I curve would, in this range, be controlled by the real a.h.p. membrane conductance and would thus be steeper than the calculated curve. With a distribution of the a.h.p. conductance over the soma and a large part of the dendritic membrane, the calculated a.h.p. current will be smaller than that which actually opposes the injected current in the real cell. However, by analogy with the effect of the a.h.p. distribution on the a.h.p. reversal level (Kernell, 1971) this effect would be rather small and comparable to other uncertainties in the calculations. In the model it was also assumed that the threshold for spike initiation was constant for successive spikes. In the real neurones, a difference was found in the threshold current for successive spikes (section VIII). This difference was usually small for the first two spikes (less than 0·5 nA, Fig. 11), and omission of this factor did not affect the computed f/I curves to any significant degree.

From these considerations it is clear that the computed f/I curves cannot be expected to correspond exactly with the experimental data. However, the good agreement between the predicted and experimental curves demonstrate that the a.h.p. is of the right magnitude and time course to account for the shape and slope of the first interval f/I curve over a considerable frequency range. At high frequencies ($>$ 200–300 impulses/sec) other factors which influence the early voltage trajectory (e.g. the spike conductance and the delayed depolarization current) will of course also be of importance.

The experimental f/I curves for the interspike intervals succeeding the first were also compared with the a.h.p. properties. Since complete preceding intervals are necessary for the calculation of later intervals, this comparison was performed with an entirely theoretical neurone model based on the a.h.p. properties. This model gave first interval f/I curves and interspike voltage trajectories which were very similar to those of real DSCT neurones (Fig. 8). With linear superposition of a.h.p.s following successive spikes (Gustafsson & Zangger, 1978), the model behaviour for the later intervals was also quite similar to that of real neurones. As in the DSCT cells, there was a gradual extension of the lower leg of the f/I curve up to higher frequencies, giving a linear steady state f/I curve for later intervals. There was also a change in the slope of the lower leg of the f/I curve between successive intervals both in the

model and in the real cells. In DSCT neurones with a.h.p. depression this slope change was small and at some current strengths there was also a negative adaptation, i.e. later intervals shorter than the first one. Similar curves were also obtained in the model if an a.h.p. depression was introduced in the equations. The model interspike voltage trajectory changes during adaptation were also quite similar to those in real cells both with and without depression.

There were certain discrepancies between the f/I curves of real neurones and the curves obtained with the model with linear a.h.p. summation. The model gave a steady state f/I curve with approximately the same slope as the lower leg of the curve for the third interval. In the real neurones there was an additional adaptation represented by a slope change from the third to the 0·2 sec interval curve. On the other hand, the slope change between the first and the third interval curves was much the same in the model as in real neurones. This indicates that a.h.p. summation can account for the adaptation in real neurones down to a frequency represented by the extension of the lower leg of the third interval curve. This frequency was usually reached within the first ten intervals, as would be expected if a.h.p. summation was important for this phase of the adaptation (cf. Fig. 5 and Gustafsson & Zangger, 1978, Fig. 6). Even at high current intensities the major part of the adaptation from the first to the 0·2 sec interval was represented by frequencies above the extension of the third interval curve. Thus, a.h.p. summation seems to be quantitatively the most important factor determining the initial adaptation in DSCT cells.

High frequency negative adaptation was present in all but one of the cells with a.h.p. depression. This type of behaviour has been described in pyramidal tract cells (Koike, Mano, Okada & Oshima, 1970; Calvin & Sypert, 1976) and rubrospinal neurones (Hultborn, H., Murakami, F. & Tsukahara, N., in preparation). The model with a.h.p. depression displayed a similar negative adaptation at high frequencies. This behaviour of the model depends on two aspects of the a.h.p. properties which have not been unequivocally proven. The a.h.p. conductance has to decay in two phases, an early rapid and a late slow one (Gustafsson *et al.* 1978) and both phases of the a.h.p. conductance should be depressed proportionally (Gustafsson & Zangger, 1978). At short interspike intervals under such circumstances the a.h.p. conductance following the second spike will be smaller during the initial phase than that following the first spike, but larger during the remaining part of the a.h.p. This statement can be exemplified as follows. Assume that the a.h.p. conductance is 1·0, 0·10 and $0{\cdot}08 \times 10^{-6}$ S at 1, 5 and 9 msec after the first spike respectively. The net a.h.p. conductance given by the second spike is reduced to half, i.e. to 0·5 and 0·05 and $0{\cdot}04 \times 10^{-6}$ S at the given intervals after the second spike. With an interspike interval of 4 msec and a linear a.h.p. summation, the total a.h.p. conductance following the second spike will be 0·6 and $0{\cdot}13 \times 10^{-6}$ S at 1 and 5 msec after the second spike respectively. Thus the second a.h.p. conductance will be initially smaller than the first but larger later on. The injected current will therefore displace the membrane potential towards the threshold voltage more easily just after the second spike than after the first, giving a second interval shorter than the first. It is obvious that this behaviour of the model rests upon the assumption of a large initial a.h.p. conductance, as obtained when it is calculated from the a.h.p. voltage (Gustafsson *et al.* 1978).

The high frequency negative adaptation in pyramidal tract cells has been ascribed to an increase in the delayed depolarization following the second and succeeding spikes (Calvin & Sypert, 1976). An increase in this DD can be observed also in DSCT cells (Fig. 11 in Gustafsson & Zangger, 1978), and a negative adaptation can be obtained with the model version without a.h.p. depression, provided that the delayed depolarization current for the second spike is increased sufficiently. However, there are reasons to believe that the negative adaptation in DSCT neurones is due to a.h.p. depression rather than to an increase in delayed depolarization. First, the negative adaptation was present only in cells with a.h.p. depression, while an increase in delayed depolarization was observed also in cells without depression. Secondly, the f/I curves at lower frequencies are unaffected when a high frequency negative adaptation is produced by a delayed depolarization increase in the model. This results in a clear change in the slope of the f/I curve from the first to the second interval which is not found in DSCT neurones with a negative adaptation or in the model with a.h.p. depression. Thirdly, the interspike voltage trajectories given by the model with an increased delayed depolarization are quite different from those of the real neurones while the model with a.h.p. depression gives voltage trajectories as in the real cells. All this points to a causal relationship between the a.h.p. depression and the high frequency negative adaptation in some DSCT neurones. It should be pointed out that in neurones with a.h.p. depression the smaller a.h.p. conductance after the second spike will result in an augmented delayed depolarization, even if the delayed depolarization current is unchanged.

This discussion leads to the conclusion that the conductance process underlying the a.h.p. plays a major role in the regulation of repetitive firing in DSCT neurones. Thus, the firing in these cells is controlled by the postspike refractoriness in the manner originally proposed by Adrian & Zotterman (1926) and later by Kernell (1968). It is interesting to note that the dissimilarities in the firing behaviour of DSCT neurones and spinal motoneurones are reflected in small differences in the a.h.p. properties of these cells. The steeper f/I slopes and the negative adaptation in some DSCT cells is related to their smaller a.h.p. (Gustafsson *et al.* 1978) and the presence of an a.h.p. depression (Gustafsson & Zangger, 1978) which is not found in motoneurones. The less pronounced upward deviation from the lower leg of the first interval f/I curve and the absence of an intersection of the second and third interval f/I curves in the DSCT cells is correlated with the lack of a plateau phase in the decay of the a.h.p. conductance (cf. Baldissera & Gustafsson, 1974*a*). In motoneurones, an upward deviation of the steady state f/I curve at high current intensities is often observed (Kernell, 1965*c*). The plateau in the decay of the a.h.p. conductance in combination with an a.h.p. summation which is considerable less than linear seems to account for this effect (Baldissera & Gustafsson, 1974*c*; Baldissera, Gustafsson & Parmiggiani, 1976, 1977).

The present analysis has been concerned exclusively with the intrinsic mechanism for the regulation of repetitive firing in DSCT neurones. The timing of impulses in a neuronal output might depend also on temporal patterns in the synaptic input. This aspect of the firing of DSCT neurones has been considered by Walløe, Jansen & Nygaard (1969).

We are indebted to Professor A. Lundberg for his interest and support during this study. The work was supported by the Swedish Medical Research Council (Project nos. 04767 and 00094) and the Swiss National Foundation.

REFERENCES

ADRIAN, E. D. & ZOTTERMAN, Y. (1926). The impulses produced by sensory nerve-endings. Part 2. The response of a single end-organ. *J. Physiol.* **61**, 151–171.

BALDISSERA, F. & GUSTAFSSON, B. (1974*a*). Afterhyperpolarization conductance time course in lumbar motoneurones of the cat. *Acta physiol. scand.* **91**, 512–527.

BALDISSERA, F. & GUSTAFSSON, B. (1974*b*). Firing behaviour of a neurone model based on the afterhyperpolarization conductance time course. First interval firing. *Acta physiol. scand.* **91**, 528–544.

BALDISSERA, F. & GUSTAFSSON, B. (1974*c*). Firing behaviour of a neurone model based on the afterhyperpolarization conductance time course and algebraic summation. Adaptation and steady state firing. *Acta physiol. scand.* **92**, 27–47.

BALDISSERA, F., GUSTAFSSON, B. & PARMIGGIANI, F. (1976). A model for refractoriness accumulation and secondary range firing in spinal motoneurones. *Biological Cybernetics* **24**, 61–65.

BALDISSERA, F., GUSTAFSSON, B. & PARMIGGIANI, F. (1977). Saturation of a.h.p. conductance summation as a mechanism for 'secondary range' firing in spinal motoneurones. *Brain Res.* (In press.)

CALVIN, W. H. & SYPERT, G. W. (1976). Fast and slow pyramidal tract neurons: an intracellular analysis of their contrasting repetitive firing properties in the cat. *J. Neurophysiol.* **39**, 420–434.

ECCLES, J. C. (1957). *The Physiology of Nerve Cells.* Baltimore: The Johns Hopkins Press.

EIDE, E., FEDINA, L., JANSEN, J., LUNDBERG, A. & VYKLICKÝ, L. (1969). Properties of Clarke's column neurones. *Acta physiol. scand.* **77**, 125–144.

GRANIT, R., KERNELL, D. & SHORTESS, G. K. (1963). Quantitative aspects of repetitive firing of mammalian motoneurones, caused by injected currents. *J. Physiol.* **168**, 911–931.

GRANIT, R., KERNELL, D. & LAMARRE, Y. (1966*a*). Algebraical summation in synaptic activation of motoneurones firing within the 'primary range' to injected currents. *J. Physiol.* **187**, 379–399.

GRANIT, R., KERNELL, D. & LAMARRE, Y. (1966*b*). Synaptic stimulation superimposed on motoneurones firing in the 'secondary range' to injected current. *J. Physiol.* **187**, 401–415.

GUSTAFSSON, B. (1974). Afterhyperpolarization and the control of repetitive firing in spinal neurones of the cat. *Acta physiol. scand.*, suppl. 416.

GUSTAFSSON, B., LINDSTRÖM, S. & TAKATA, M. (1972). Repetitive firing in dorsal spinocerebellar tract neurones. *Brain Res.* **47**, 506–509.

GUSTAFSSON, B., LINDSTRÖM, S. & TAKATA, M. (1978). Afterhyperpolarization mechanism in the dorsal spinocerebellar tract cells of the cat. *J. Physiol.* **275**, 283–301.

GUSTAFSSON, B. & ZANGGER, P. (1978). Effect of repetitive activation on the afterhyperpolarization in dorsal spinocerebellar tract neurones. *J. Physiol.* **275**, 303–319.

ITO, M. & OSHIMA, T. (1965). Electrical behaviour of the motoneurone membrane during intracellularly applied current steps. *J. Physiol.* **180**, 607–635.

KERNELL, D. (1965*a*). Synaptic influence on the repetitive activity elicited in cat lumbosacral motoneurones by long-lasting injected currents. *Acta physiol. scand.* **63**, 409–410.

KERNELL, D. (1965*b*). The adaptation and the relation between discharge frequency and current strength of cat lumbosacral motoneurones stimulated by long-lasting injected currents. *Acta physiol. scand.* **65**, 65–73.

KERNELL, D. (1965*c*). High-frequency repetitive firing of cat lumbosacral motoneurones stimulated by long-lasting injected currents. *Acta physiol. scand.* **65**, 74–86.

KERNELL, D. (1965*d*). The limits of firing frequency in cat lumbosacral motoneurones possessing different time course of afterhyperpolarization. *Acta physiol. scand.* **65**, 87–100.

KERNELL, D. (1968). Repetitive impulse discharge of a simple neurone model compared to that of spinal motoneurones. *Brain Res.* **11**, 685–687.

KERNELL, D. (1971). Effects of synapses of dendrites and soma on the repetitive impulse firing of a compartmental neuron model. *Brain Res.* **35**, 551–555.

KERNELL, D. & SJÖHOLM, H. (1973). Repetitive impulse firing: comparisons between neurone models based on 'voltage clamp equations' and spinal motoneurones. *Acta physiol. scand.* **87**, 40–56.

KOIKE, H., MANO, N., OKADA, Y. & OSHIMA, T. (1970). Repetitive impulses generated in fast and slow pyramidal tract cells by intracellularly applied current steps. *Expl Brain Res.* **11**, 263–281.

KUNO, M. & MIYAHARA, J. T. (1968). Factors responsible for multiple discharge of neurons in Clarke's column. *J. Neurophysiol.* **31**, 624–648.

MACGREGOR, R. J. & SHARPLESS, S. K. (1973). Repetitive discharge of a simple neuron model with accumulation of afterhyperpolarization conductance. *Brain Res.* **64**, 387–390.

MAURITZ, K.-H., SCHLUE, W. R., RICHTER, D. W. & NACIMIENTO, A. C. (1974). Membrane conductance course during spike intervals and repetitive firing in cat spinal motoneurones. *Brain Res.* **76**, 223–233.

SCHWINDT, P. C. (1973). Membrane-potential trajectories underlying motoneuron rhythmic firing at high rates. *J. Neurophysiol.* **36**, 434–449.

SCHWINDT, P. C. & CALVIN, W. H. (1972). Membrane-potential trajectories between spikes underlying motoneurone firing rates. *J. Neurophysiol.* **35**, 311–325.

SCHWINDT, P. C. & CALVIN, W. H. (1973*a*). Equivalence of synaptic and injected current in determining the membrane potential trajectory during motoneuron rhythmic firing. *Brain Res.* **59**, 389–394.

SCHWINDT, P. C. & CALVIN, W. H. (1973*b*). Nature of conductances underlying rhythmic firing in cat spinal motoneurons. *J. Neurophysiol.* **36**, 955–973.

WALLØE, L., JANSEN, J. K. S. & NYGAARD, K. (1969). A computer simulated model of a second order sensory neurone. *Kybernetik* **6**, 130–140.